

Optically active defects in SiO₂: The nonbridging oxygen center and the interstitial OH moleculeT. Bakos,^{1,*} S. N. Rashkeev,¹ and S. T. Pantelides^{1,2}¹*Department of Physics and Astronomy, Vanderbilt University, Nashville, Tennessee 37235, USA*²*Solid State Division, Oak Ridge National Laboratory, Oak Ridge, Tennessee 37831, USA*

(Received 7 December 2003; revised manuscript received 11 May 2004; published 10 August 2004)

Irradiation of high-OH containing amorphous SiO₂ is known to introduce a broad absorption band at 4.8 eV and an associated sharp photoluminescence band in the visible red domain, at 1.9 eV. Both absorption and luminescence bands have been unambiguously attributed to the nonbridging oxygen (NBO) center, a common defect in irradiated SiO₂. Using results of first-principles calculations we show that the NBO center and the interstitial OH molecule (OH_i) may both be responsible for the observed absorption and luminescence bands. Although the absorption spectra of the two defects are very similar, their luminescence spectra are different, but overlapping. We found that the NBO center has a sharp luminescence line centered around 1.8 eV in the visible red, whereas OH_i molecules have a wide emission spectrum ranging from the infrared (0.8 eV) to visible red (1.8 eV). Investigation of the results show that the difference in the emission spectra is due to the different extent of atomic and electronic relaxations around the two defects: in the case of the NBO, site-independent *electronic relaxations* are responsible for the defect emitting a photon only at a particular energy, whereas in the case of OH_i molecules an interplay between site-dependent *atomic and* (therefore site-dependent) *electronic relaxations* result in a wide emission spectrum. A further, intriguing result is that both defects show similar vibrational and polarization properties, therefore their contribution to the red luminescence band of irradiated amorphous SiO₂ may not have been decoupled in previous studies.

DOI: 10.1103/PhysRevB.70.075203

PACS number(s): 71.55.Jv, 61.72.Bb, 78.20.-e, 78.55.Qr

I. INTRODUCTION

Investigation of the optical spectra of defects in oxides and semiconductors plays an important role in the study of defect structures, often complementing other techniques such as, e.g., electron paramagnetic resonance (EPR) spectroscopy. In particular, parameters extracted from optical absorption (OA) and photoluminescence (PL) spectra (e.g., location and width of optical bands, transition matrix elements or lifetimes of excited states) supply useful information about the electronic structure of defects.

In this paper we present a detailed theoretical investigation of the optical properties of two particular defects, the nonbridging oxygen (NBO) center and the interstitial hydroxyl (OH_i) molecule. The NBO center is generally believed to be the defect that is responsible for a broad optical absorption (OA) band centered around 4.8 eV and a subsequent sharp photoluminescence (PL) band centered at 1.9 eV.^{1,2} The OH_i has not been associated with any experimental signature. However, an elementary analysis of the expected energy levels of the two defects suggests that they may have a similar structure (both have a “dangling oxygen” with an unpaired electron in the 2*p* shell). This conjecture proved rewarding in that we unveiled a number of intriguing similarities and differences between the two defects, suggesting new experiments to elucidate the nature of their optical spectra.

We first analyze the optical properties of the NBO center, which is an oxygen atom bound to only one silicon with an unpaired electron in its nonbonding 2*p* orbital. The NBO was first observed in EPR measurements of irradiated, high OH-containing SiO₂ glass.³ The EPR signal of the NBO center was found to correlate reasonably well with the 1.9 eV PL

intensity, although it was suggested that other defects may also contribute to the luminescence.⁴ Also, several cluster calculations argued that the electronic structure of the NBO allows for the observed PL line.⁵ Direct optical excitation in the 1.9 eV band is also possible, though the efficiency of such a process is very low. The excitation energy in this case is centered around 2.0 eV.

We show that the presence of a large Stokes shift, i.e., the ~2.9 eV difference between the peak OA and PL energies, in the NBO defect is entirely due to slow, nonradiative electronic relaxations inside the SiO₂ valence band. During this electronic relaxation process, a deep valence hole, which has been created in the excitation process “bubbles up” to the valence band edge by a cascade of one-phonon electronic transitions which is unique to the solid state because it requires a continuum of higher-lying electronic states to be present. This electronic relaxation process—a form of “electronic” Franck-Condon (FC) shift—is suggested to have broad applicability in determining the optical behavior of defects in various media.⁶ Thus, the “electronic” FC shift would be a complementary process beside atomic relaxations that are usually attributed to determine the Stokes shift in defects.

In contrast to the NBO atom OH interstitials are difficult to observe directly in experiment, because of their high reactivity and diffusivity. (The NBO center is also reactive, but localized.) However, as an iterim product, they may be created by the radiation induced dissociation of water molecules⁷ or by water molecules reacting with NBO centers or peroxy radicals in the oxide.⁸ Direct EPR observation of interstitial neutral OH groups was possible only in sodium-silicate glasses with water content above 2% by weight.⁸

We show that the OH_i has a very similar electronic structure and optical cycle, except for two important differences.

First, although the OH_i has a virtually identical absorption spectrum to the NBO, it may luminesce at a range of energies including the well-known red PL band previously associated solely with NBO centers. The energy of the emitted photon depends on the local electronic environment experienced by the OH_i group. The reason for this site-dependence constitutes the second difference between the behavior of the two defects. The Stokes shift in the OH_i defect comprises a combination of electronic and atomic relaxation processes with relaxation energies dependent on the initial position of the defect in the amorphous solid. The electronic relaxation process is the same as in the NBO defect, i.e., is related to a bubbling up of a deep valence hole to the top of the valence band via a cascade of one-phonon electronic transitions. In the atomic relaxation process, the excited OH_i moves closer to a network Si atom because of Coulomb attraction. The total energy gain in both electronic and atomic relaxation processes depends on the Coulomb interaction between the deep valence hole and the excited OH_i molecule. This Coulomb interaction is determined by the distance between the OH_i molecule and the network accommodating the deep valence hole. As opposed to OH_i we found that the NBO defect does not have site-to-site variations in its geometric structure nor does it show atomic relaxations following excitation or luminescence.

The net conclusion is that both the NBO and the OH_i may contribute to the observed optical spectra (4.8 eV OA and 1.9 eV PL) that are normally attributed solely to NBO centers.

The rest of the paper is organized as follows: In Sec. II we describe briefly the necessary details of our computational approach. In Sec. III we present results of calculations for the electronic band structures and relaxation processes of the NBO and OH_i defects respectively. Subsequently, in Sec. IV we give a detailed account of the experimental observations that accompany red PL and show that they are consistent with both defects. A summary of the main conclusions of this work is given in Sec. V.

II. COMPUTATIONAL METHOD

The present calculations are based on first-principles density functional theory (DFT), the generalized gradient approximation for the exchange-correlation energy, ultrasoft pseudopotentials, supercells, and plane waves.^{9,10} The pseudopotentials used for the present study have been thoroughly tested in earlier work on a variety of Si–O–H systems.^{11–13} As in that work, the energy cutoff for the basis set was 24 Ry, and integrations over the Brillouin zone were done using the Monkhorst-Pack scheme with only one special k-point in the relevant irreducible wedge.¹⁴

The calculations were performed for 72-atom α -quartz and 72-atom amorphous SiO_2 supercells. The amorphous structures were generated by using the Monte Carlo bond-switching method (see Refs. 15 and 16 for details) and relaxed until the total energy was minimized (the force on each atom is smaller than a tolerance, namely 0.1 eV/Å). The size of supercells (~ 10 Å) is large enough to neglect the interaction of a defect with its periodic images. The electronic tran-

sition energies were calculated by comparing the total energies of the initial and final (excited) states of the system where the excited states were created by manually fixing the band occupancy numbers. For studying charged defects we introduced a homogeneous negative (positive) background when removing (adding) electrons in the supercell and added the Makov-Payne correction terms to the total energy.¹⁷

The diffusion barrier for OH_i was determined by calculating the variation in total energies of the OH_i molecule at 5 intermediate points along a trajectory connecting it with its periodic image. In these calculations only one coordinate of the diffusing OH_i was fixed, along the trajectory connecting the initial and final positions of the oxygen atom. The rest of the system was allowed to relax. This technique has been shown to work well for interstitial H_2O and O_2 molecules.¹³

Vibrational frequencies of the Si–O bonds in the NBO atom and (5)Si–OH[−] (this defect forms in the interim of the OA and PL processes of the OH_i molecule; see next section) were determined in the frozen phonon approximation.

We have also calculated the optical matrix elements for transitions from different valence levels (Ψ_b) to the (uniquely defined) defect level (Ψ_a) and evaluated the absorption coefficient (averaged over all the possible light polarizations):

$$\alpha(\omega) = \frac{4\pi e^2 \hbar^2}{\epsilon_0 m^2 \omega^2} \sum_i |\langle \Psi_a | \nabla | \Psi_b \rangle|^2 \delta(\omega + E_a - E_b). \quad (1)$$

In practical calculations δ -functions are replaced by Lorentzians with $\gamma=0.2$ eV.

III. RESULTS

A. Relaxation processes and optical properties of nonbridging oxygen atoms

We find that, in its ground state, the NBO has two levels slightly above the valence band edge (E_v); one of them is filled by two electrons while the other one is populated by only one [Fig. 1(c), left diagram]. These levels are nonbonding $2p$ orbitals that naturally lie very close to E_v , which is made up of similar orbitals of the fully coordinated O atoms. The similar character of the defect states and the orbitals constituting the valence band edge suggests that optical excitations from the valence band edge are suppressed and more likely to originate from deeper valence levels. This observation is consistent with the fact that the OA spectrum is a broad band and is centered at an energy much higher than the position of the defect levels (4.8 eV).¹⁸

To find the possible initial states for optical excitation, we calculated the optical matrix elements for transitions from deep valence levels to the partially occupied level of the NBO. Our results show that these matrix elements are approximately constant when the initial state belongs to the upper half (0–6 eV region) of the valence band. This valence band region is composed mainly of a combination of Si sp^3 and a combination of the O $2p_x$ and $2p_y$ states where the orientation of the y axis is in the Si–O–Si plane perpendicular to the Si–Si line, i.e., the O $2p_y$ states are only weakly overlapping with Si sp^3 [see Fig. 1(b) and Ref. 19 for details].

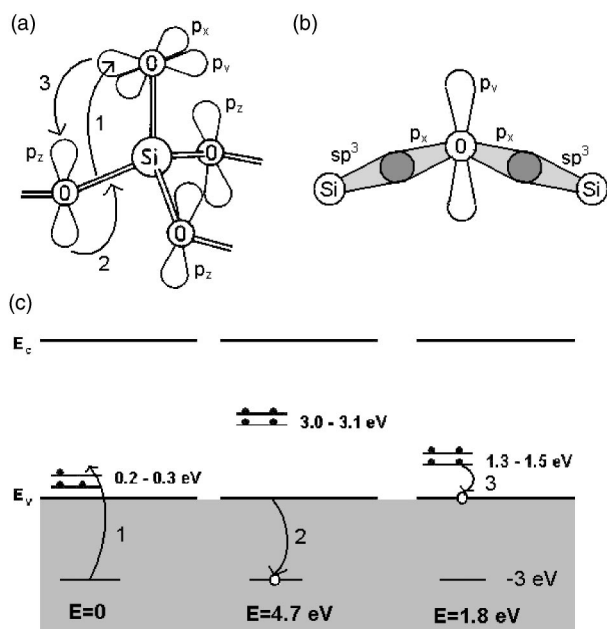


FIG. 1. (a) Schematics of the three main electronic processes responsible for the absorption and photoluminescence spectra of NBO. (b) O₂p orbitals in the three-center Si-O-Si bond. $2p_x$ lies along the Si-O line strongly overlapping with Si sp^3 , $2p_y$ is in the Si-O-Si plane only weakly overlapping with Si sp^3 . The nonbonding $2p_z$ orbitals (not drawn) are perpendicular to the figure. (c) One-electron energy level diagram of the NBO just before the corresponding transitions. The total energies of the system in these states (relative to the ground state) are shown in the bottom.

Figure 2 shows the optical absorption coefficient as a function of $E = \hbar\omega - 0.3$ eV, where $\hbar\omega$ is the photon energy, and 0.3 eV is the distance between the top of the valence band and the unoccupied nonbonding $2p$ orbital of the NBO defect. We plotted α as a function of E because we are interested to identify the dominant initial states. The calculations for the optical absorption were performed in the one-electron approximation whereas we will later see that the excitation energy entails significant many-body effects (e.g., Hubbard U). Since the matrix elements are approximately constant in the $E = 0 - 6$ eV region, the optical absorption curve nearly coincides with the density of states (DOS) curve

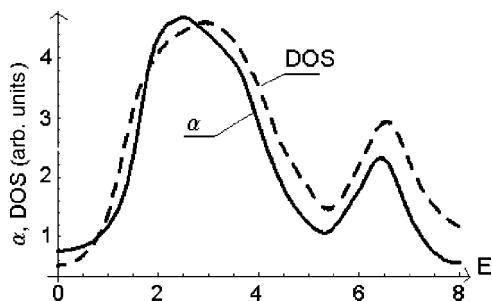


FIG. 2. Absorption coefficient $\alpha(\hbar\omega - 0.3$ eV) for transitions into the unoccupied level of the NBO defect compared with the DOS for the valence band (zero of energy for DOS corresponds to E_v , the energy axis is directed towards decrease of the energy). The units for both of the curves are arbitrary.

(cf. Fig. 2). Therefore, the band region near the DOS maximum (i.e., about 3 eV below E_v) gives the main contribution to the optical absorption spectrum of the NBO.

The experimental value of the excitation energy (4.8 eV) is higher than what one would expect to obtain from the one-electron energy level positions of the participating states (i.e., 0.3+3.0 eV). This difference is a result of many-body effects (e.g., Hubbard U) that are not taken into account in the calculation of the one-electron energy eigenvalues. These many-body effects are included when one calculates the optical transition energies as a difference between the total energies in the final and initial states. Indeed, subtracting the total energy of the ground state NBO supercell from the total energy of the supercell containing the excited defect and a valence hole at ~ 3 eV below E_v , we find 4.7 eV for the energy of excitation, in good agreement with the experimental 4.8 eV. The variation in excitation energy with respect to the position of the NBO atom within the supercell was within the accuracy of our calculations.

After the excitation process [process 1 in Figs. 1(a) and 1(c)], we are left with a hole in the valence band (at ~ 3 eV below E_v) and a negatively charged NBO atom. The NBO $2p$ levels experience a large shift due to on-site repulsion: the one-electron energy spectrum calculated in the excited state shows that these levels shift up and are now located at ~ 3 eV above E_v . In a subsequent process an electron has to deexcite from one of these defect orbitals or higher lying valence band states to the level of the deep valence hole. However, the calculated optical matrix elements for these deexcitations are small since the defect and higher-lying valence orbitals and the deep hole state have substantial p -character. As a result, it is easier for the system to lower its energy by the deep valence hole “bubbling up” to the valence band edge in a phonon-assisted mechanism [process 2 in Figs. 1(a) and 1(c)]. Although we did not investigate the participating phonon modes in detail, for the purpose at hand it is sufficient to note that the phonon-assisted bubbling up of the hole is a nonradiative process which is slow in comparison with the characteristic times typical for the electronic transitions. In the following we will refer to this process as a “slow, nonradiative electronic relaxation,” since it actually involves a charge redistribution within the valence band.

In order to study the charge distribution around the deep hole and the corresponding charge relaxation mechanism, we plotted the difference between the charge densities of a supercell containing the deep hole state and a supercell containing the hole on the top of the valence band (Fig. 3). During the electronic relaxation process the charge is shifting from the dark shaded clouds into the light shaded areas. This effect is most pronounced around the oxygen atoms adjacent to the Si atom connected to the NBO and at the NBO itself. Apparently, the participating electronic states are delocalized (they are “smeared out” around at least four O atoms, although a similar, but smaller charge shift can be observed around *all* network O atoms). We also notice that the light shaded clouds that represent the positive charge associated with the deep hole (i.e., the negative charge that is “missing” from the supercell that includes the deep hole) are aligned in the Si-O-Si plane. These clouds are the actual O $2p_y$ states that—weakly interacting with Si sp^3 states—contribute in

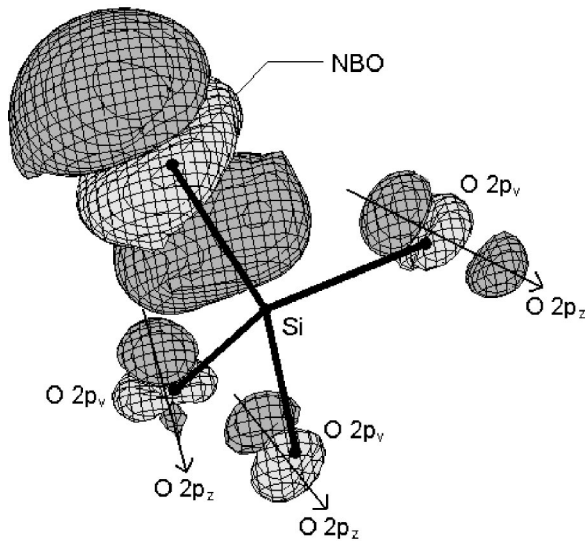


FIG. 3. Difference of the charge densities of the supercell before and after electronic relaxation. The dark areas represent the volume that contains more negative charge before relaxation. During the relaxation process, this charge is transferring to the light colored areas. The dark areas can be identified as the O $2p_z$ states that are filled before relaxation whereas the light areas mainly consist of the O $2p_y$ states that constitute the deep valence hole state and are therefore unoccupied. After the relaxation process the situation reverses: the O $2p_z$ states (dark clouds) become unoccupied while the O $2p_y$ states (light clouds) become occupied.

the formation of the upper part of the valence band. In contrast, the dark shaded clouds are oriented perpendicular to the Si–O–Si plane (arrows in Fig. 3). These clouds represent the non-bonding O $2p_z$ states that make up the top valence band orbitals. The orbital character of the deep hole and the states that form the top of the valence band confirms our previous assumption, that the electronic relaxation involves transitions mainly between oxygen p -like orbitals. The physical charge redistribution within the valence band alters the local electrostatic potential around the NBO atom. As a result, the defect energy levels are again shifted, albeit by a lesser extent than following the excitation process, since the total negative charge located at the NBO defect does not change.

During the initial excitation and subsequent electronic relaxation processes the system is nearly “frozen,” i.e., no change in the atomic positions could be observed. The total energy difference between the initial and final stage of the electronic relaxation process is 2.9 eV which equals to the Stokes shift associated with the studied OA/PL process.

The last stage of the NBO associated OA/PL cycle is the deexcitation of an electron from the NBO defect level in the gap to the hole state located at the top of the valence band [process 3 in Figs. 1(a) and 1(c)]. Comparing total energy differences, a PL energy of 1.8 eV is obtained, which is again in excellent agreement with experiments.^{1,2}

A reverse process, namely, the electronic excitation from the top of the valence band to the NBO defect level in the gap, also exists. Experimentally it was found that the absorption band corresponding to this process is centered at 2.0 eV.^{1,2} In this case no electronic relaxations are present,

therefore the PL is exactly the reverse of the OA process and naturally has the same energy. Since the participating electronic states are almost purely O $2p$ states, this OA/PL cycle will have a lower intensity than the cycle where the initial excitation occurs at 4.8 eV.

In this subsection we have shown that the NBO defect has a main absorption peak at 4.7 eV and an associated PL band at 1.8 eV. The relatively large Stokes shift is exclusively due to slow, nonradiative electronic relaxations inside the valence band.

B. Relaxation processes and optical properties of OH_i molecules in *a*-SiO₂

Using the same calculational tools and approaches, we have identified another defect—interstitial OH groups—which has a very similar optical signature. Since the 4.8 eV OA and the 1.9 eV PL is primarily observed in high-OH containing irradiated oxides with an intensity increasing with increasing OH content,²⁰ we suggest that this defect may also contribute to the optical processes in question.

Neutral OH_{*i*}-s have two distinct equilibrium positions in *a*-SiO₂; they are either H-bonded to a network O atom or O-bonded to a network Si atom by a dipole interaction. This weak binding can be understood in the ionic picture of SiO₂; network O-s accumulate most of the negative charge and therefore they attract the positive (H) end of the OH dipole. Similarly, network Si atoms are somewhat positively charged; therefore, they attract the O atom of the OH dipole. In each case it costs ~ 0.3 eV to move the OH group in the middle of the void, where it is approximately equidistant from all nearest oxygens and silica.

A neutral OH molecule has two levels in the band gap that are of oxygen $2p$ character just like the NBO [Fig. 4(c)]. Since the oxygen atom is bound to H, not to Si as in the case of the NBO defect, these p -levels do not need to be close to E_v . In order to find the most probable candidate states in the SiO₂ valence band where an excitation may originate from, we have again calculated the optical matrix elements for the transitions from deep valence bands to the OH_{*i*} partially occupied level. The result is similar to the case of the NBO, namely that the matrix elements are approximately constant for initial states lying within the upper part (0–6 eV, with $E_v=0$) of the valence band. The absorption coefficient α as a function of $E=\hbar\omega-1.3$ eV clearly shows that the dominant contribution to the excitation spectrum is coming from valence orbitals close to the DOS maximum, namely, from the region ~ 2.5 –3.5 eV below E_v (Fig. 5). Comparing total energy differences we find that the excitation energy of the initial OA process occurs in the 4.7–5.0 eV range depending on the initial position of the OH_{*i*}. This excitation is represented as process 1 in Fig. 4.

The excitation process produces a deep valence hole (as in the case of the NBO) and a negatively charged OH_{*i*} (OH⁻). Analysis of the optical matrix elements for transitions from higher valence or defect levels to the deep hole state again suggests that optical de-excitation has low probability. Similarly to the case of the NBO, the deep hole state prefers to “bubble up” to the top of the valence band in a

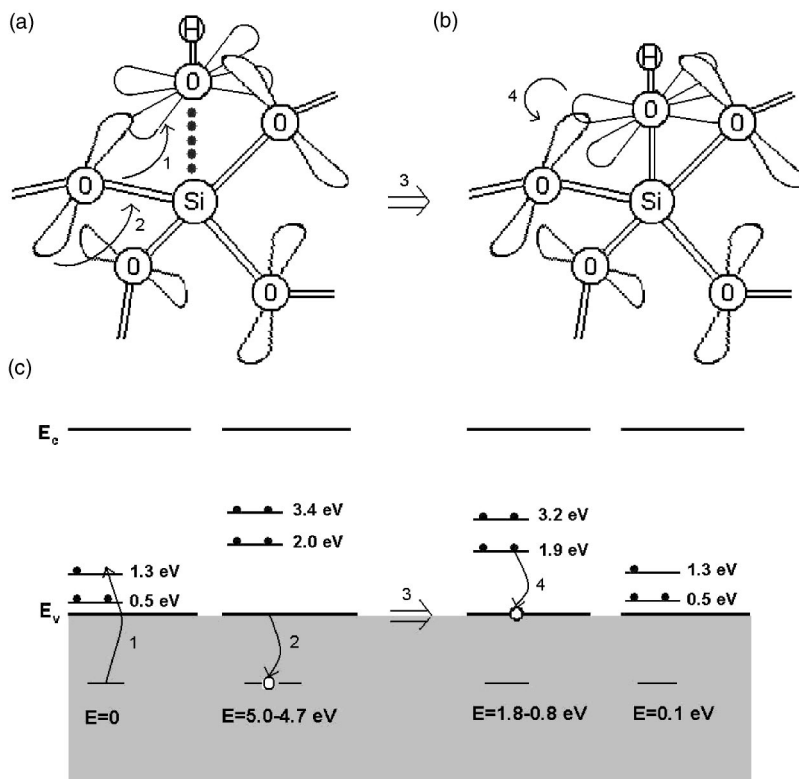


FIG. 4. Schematics of the three main electronic processes (1, 2, and 4) and the atomic relaxation process (3) responsible for the absorption and photoluminescence spectra of OH_i. (a) Schematics and electronic transitions in OH_i. (b) Schematics and the PL transition in (5)Si–OH[−]. This defect forms as the charged OH_i relaxes and binds to a network Si. (c) One-electron energy level diagram of the OH just before the corresponding transitions. The total energies of the system in these states (relative to the ground state) are shown in the bottom.

slow, nonradiative phonon-assisted process (process 2 in Fig. 4). The electronic states participating in this relaxation process again have mainly O *2p*-character as it can be seen from a charge density difference plot (Fig. 6).

Despite the similarity in the physical nature of the excitation and electronic relaxation processes we find a very sensitive site-dependence for the energy release in the electronic relaxation process. To understand this phenomenon first we analyze the variation in excitation energies and compare the results with similar energies obtained for quartz (Table I).

We found that the reason for the decrease in excitation energies in smaller voids is that the OH_i is initially more “squeezed” to the network, therefore the overlap between the

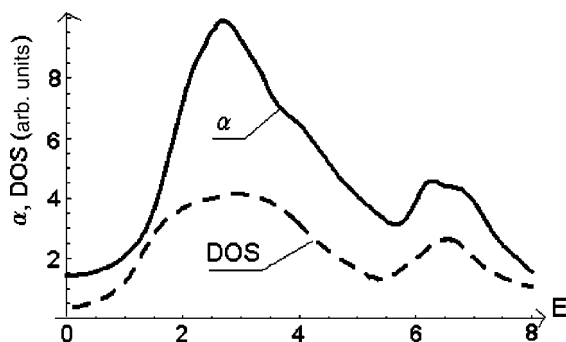


FIG. 5. Absorption coefficient $\alpha(\hbar\omega - 1.3 \text{ eV})$ for transitions into the lowest unoccupied level of the OH defect compared with the DOS for the valence band (zero of energy for DOS corresponds to E_v , the energy axis is directed towards decrease of the energy). The units for both of the curves are arbitrary. The DOS is scaled by the same factor as in the case of the NBO defect, i.e., $\alpha(\text{OH}_i) \approx 2 * \alpha(\text{NBO})$.

electronic wave functions of the states participating in the excitation process is greater than in the larger voids of the oxide. The greater overlap leads to a lesser extent of charge separation between the network and the OH[−], i.e., the excited electron will have a part of its wavefunction still smeared around neighboring network atoms. The smaller charge shift leads to smaller Hubbard *U* effects that also reduce the total energy of the excited states. In larger voids, however, almost all of the excited electron will be located around the O atom of the OH[−], resulting in larger Hubbard *U*-s and excitation energies. To justify this assumption, we have calculated the increase in total charge caused by optical excitation inside a sphere having the cutoff radius ($R = 1.55 \text{ \AA}$) around the O atom of the OH molecule in voids of different sizes. As the data in Table I show the charge separation (i.e., the part of the electron localized over the OH_i) following the OA is smaller if the OH_i resides in the smaller voids. In the case of quartz, the excitation energy is higher than in *a*-SiO₂, possibly because of differences in the band structure of the two materials. The small extent of charge separation, however, fits the tendency observed for *a*-SiO₂.

Table I shows that the electronic relaxation energy, which accounts for part of the Stokes shift, increases with decreasing void size. The site-sensitive nature of the relaxation energy is connected to the incomplete charge separation resulting from the excitation. Figure 6 shows that, upon the electronic relaxation process, there is a significant change in the charge density distribution around the OH[−] molecule and adjacent network O atoms. In the case of the OH[−] a part of the binding O *2p_x* electron is being transferred to nonbonding O *2p_y* and *2p_z* orbitals. For network O atoms we observe a similar effect as in the case of the NBO—the charge transfers from O *2p_y* to nonbonding O *2p_z* orbitals. This charge redis-

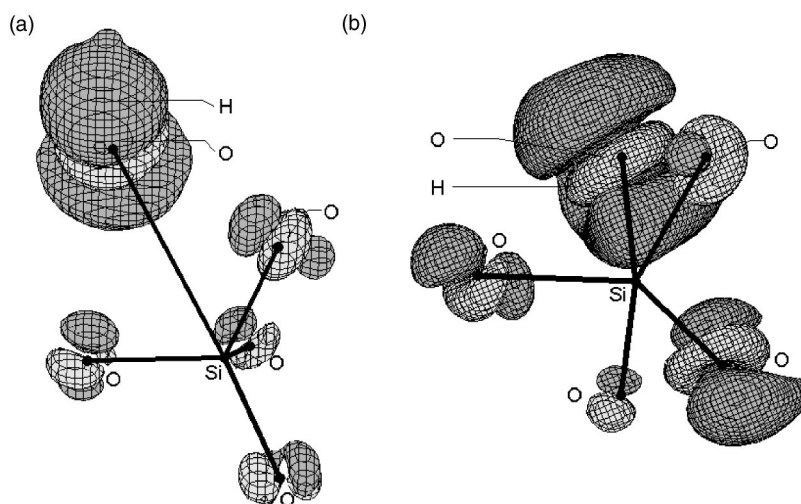


FIG. 6. Charge density difference of the supercells before and after electronic relaxation at the OH_i . As in the case of the NBO, the dark areas contain more charge before relaxation, this charge is transferring to the light colored areas during the relaxation process. The dark areas are mainly the O $2p_z$ states that are filled before relaxation whereas the light areas are the O $2p_y$ states that contribute to the deep valence hole state and are therefore unoccupied. After the relaxation process the situation reverses: the O $2p_z$ states (dark clouds) will be unoccupied and the O $2p_y$ (light clouds) will be occupied. (a) Results for OH_i in a $a \sim 6$ Å void. (b) Results for OH_i in $a \sim 3.5$ Å void. The extent of charge transfer during electronic relaxation is larger in smaller voids.

tribution is more pronounced in smaller voids as can be seen comparing the two charge density difference plots in Fig. 6. The larger extent of the charge shift results in larger energy gains once the electron is transferred from one state to the other.

In the case of the OH_i defect, there are also significant atomic relaxations (process 3 in Fig. 4) following excitation. This atomic relaxation is a result of a Coulomb electrostatic attraction between the OH group (negatively charged when an additional electron arrives to it as a result of excitation) and the Si atom. In this process the distance between the Si and the O atom from the OH group significantly decreases.

TABLE I. Variations in Si–O distance (in Å), OA, relaxation and PL energies (eV) and charge transfer (e) for the OH_i defect in voids of different diameters (Å).

Void diameter	~ 6.0	~ 5.0	~ 3.5	~ 3.5 (α -quartz)
Si–O dist. before/after relaxation	2.34/1.87	2.20/1.77	2.07/1.71	1.87/1.69
OA energy	4.9	4.9	4.8	5.0
Electronic/atomic relaxation energy	1.7/1.4	2.1/1.4	3.1/0.9	3.5/0.8
Total relaxation energy	3.1	3.5	4.0	4.3
PL energy	1.8	1.4	0.8	0.7
Charge transfer	0.59	0.56	0.46	0.45

Naturally, this process gives the largest energy gains in large voids (cf. Table I). The reason for this effect is that both the charge separation and the displacement is larger in large voids, resulting in a higher energy gain from the Coulomb interaction of the OH^- and the network accommodating the deep valence hole.

At the final stage of the atomic relaxation, the OH^- is at $\sim 1.8 \pm 0.1$ Å apart from the Si atom which is $\sim 10\%$ longer than the average network Si–O bond. As it can be seen on a two-dimensional section of the charge density defined by the Si–O–H plane, Fig. 7, the excess electron binds the OH^- to network O atoms. Investigation of the partial density of states within a sphere of the Wigner-Seitz radius around the Si, adjacent O and H atoms reveals that the binding electron is located at the Si atom and at its 5 adjacent O atoms.

After the atomic and electronic relaxation processes we have a negatively charged OH group bound to a network Si atom and a hole at the top of the valence band. The following step is the deexcitation of the excess electron from the non-bonding OH $2p$ level to the valence band edge, resulting in the emission of a photon. This luminescence process is site-dependent, with energies distributed in the range 0.8–1.8 eV (process 4 in Fig. 4 and Table I).

This PL process restores the state of the supercell to its ground state configuration, however, at the initial moment after the PL, the neutral OH molecule is closer to the network than its equilibrium position. Thus, a final atomic relaxation process (not shown in Fig. 4) takes place resulting in a further, but very small energy release (typically ~ 0.1 eV in all cases) since the interaction between the neutral OH_i and the amorphous network is weak.

It is interesting to note that the numerical values of the square of the absolute value of the optical matrix elements for transitions from the deep valence band levels to the OH_i level are about twice the matrix elements for transitions to the NBO level (the “arbitrary units” for the absorption curves

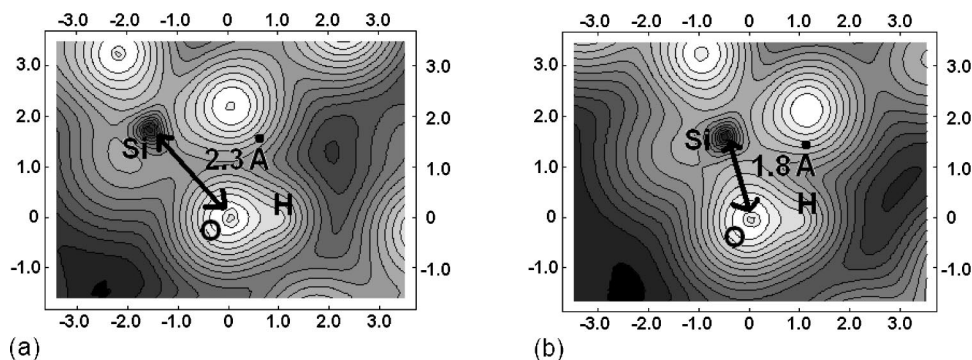


FIG. 7. Charge density contours in the Si–O–H plane: (a) before, and (b) after atomic relaxation of the OH_i defect. The excess electron becomes delocalized over the O of the OH_i and several neighboring network atoms.

in Figs. 2 and 5 are the same). Therefore once the total absorption coefficient is known, one can establish a relationship between the concentrations of the two defects.

Excitation in the luminescence band may also exist by a similar mechanism as in the case of the NBO, i.e., an electron from the top of the valence band is excited to the partially occupied O 2*p* orbital in the OH molecule. Electronic relaxations are absent in this case, however the OH_i would still relax toward a network Si atom. The presence of atomic relaxations result in a nonzero Stokes shift, unlike in the case of the NBO. The Stokes shift decreases with void size as the atomic relaxations are smaller in smaller voids.

In summary, we have shown that OH_i-s have a main OA peak around 4.7–5.0 eV and a subsequent PL band at 0.8–1.8 eV depending on the initial position of the OH_i molecule. The sum of site-dependent electronic and atomic relaxations accounts for the observed Stokes shift, with atomic relaxation energies decreasing and electronic relaxation energies increasing in smaller voids.

C. Relaxation processes and optical properties of OH_i molecules in α-quartz

Hydroxyl groups incorporate into the α-quartz crystal lattice during synthesis, where the ground silicate is usually dissolved in NaOH or Ca(OH)₂. OH groups usually attach to group III impurities (e.g., to Al) that may substitute Si atoms.²¹ Radiation may temporarily create interstitial OH groups by breaking up these bonds.

To study the site-dependent nature of the atomic and electronic relaxation processes, we have performed the same set of calculations in α-quartz as in the preceding subsection. Here we only give a summary of the results.

Since α-quartz has a more rigid structure with predominantly smaller voids, we anticipate that the effects observed in the smaller voids of *a*-SiO₂ will be magnified. We find that the dominant excitations have an energy of 5.0 eV. The subsequent electronic relaxation is indeed relatively large (3.5 eV), whereas the energy gain from atomic relaxation is small, since the OH_i moves by only about 0.18 Å toward the Si atom. The PL energy is at the lower edge of the energy range observed for *a*-SiO₂ (0.7 eV); see Table I. This result would suggest a possible way to verify the OH⁻-related OA/PL cycle experimentally. This PL line however, has not

been observed so far, possibly because of the low concentration of OH_i-s in α-quartz.

D. Stability of charged defects near the Si/SiO₂ interface

Besides their optical activity, certain defects in SiO₂ may also capture electrons or holes and become stable in the negative or positive charge state.²² This phenomenon is particularly important in the vicinity of the Si/SiO₂ interface, as electrons tunneling from the Si valence bands to defect levels in the SiO₂ or from defect levels in the SiO₂ into Si conduction bands may lead to charged defects. In this subsection we address the stability of the various charged states of the NBO and OH_i defects to determine whether they may act as charge traps if located near the Si/SiO₂ interface.

In the neutral charge state the NBO has a partially occupied level ~0.3 eV above the SiO₂ valence band edge (cf. Fig. 1). If the electron that occupies this level is removed, the localized state corresponding to the unoccupied NBO 2*p* orbital appears right at the SiO₂ valence band edge, suggesting that a positively charged state is not stable.

A positively charged OH_i is drawn closer to a network oxygen atom leading to the formation of a positively charged complex. Although there is no substantial electron density between the oxygen of the OH_i and the network O, the hole becomes delocalized on both oxygens. The change of the local potential around the OH_i and the delocalization of the hole leads to a substantial rearrangement of the oxygen one-electron energy levels, namely the now empty 2*p* level moves up to ~2.6 eV above *E_v*. This level however, is located below the Si valence band (which is ~4.6 eV above the SiO₂ valence band edge^{23b}) making it possible for an electron to tunnel into it from the Si side and render the defect neutral. Thus, a positively charged OH_i is not stable near the Si–SiO₂ interface.

In the negative charge state, the locations of the one-electron energy levels of both the NBO and OH_i defects are similar to their locations in the excited states (3.2 eV and 3.4 eV respectively, cf. Figs. 1 and 4); the differences are due to the absence of the valence hole in the present case. The locations of the one-electron energy levels however do not take into account many-body effects, as it has been pointed out in Sec. III A, and may only be regarded as approximate for the energy levels of the charged systems. To

determine whether the negative charge states of the NBO and OH_i are stable we have to compare the locations of the one-electron energy levels with the value of the Si/SiO₂ band offset resulting from the same level of theory. According to results of first-principles DFT calculations of Pantelides *et al.*,²⁴ the DFT value of the Si/SiO₂ band offset is 2.8 eV versus the experimentally observed 4.6 eV. The difference results partly from the previously mentioned inadequacy of one-electron energy levels to reproduce levels of excited states and from approximations made to the exchange-correlation potential in the framework of density functional theory. Since the one-electron energy levels of the charged defects are above the calculated value for the Si valence band edge, electrons are unlikely to tunnel into the defect levels from the Si valence band to create the negatively charged states. In the case of *n*-type Si, however, it may be possible to have a stable negatively-charged center near the interface.

Based on the locations of the one-electron energy levels compared to the Si/SiO₂ valence band offset, we conclude that both the NBO and the OH_i molecule are unlikely to act as electron or hole traps in the vicinity of the Si/SiO₂ interface, except in the case of *n*-type Si where OH_i^- may be possible. The NBO defect cannot capture a hole even in the bulk oxide. Ionizing radiation however, may create electron-hole pairs in the bulk oxide and the mobile conduction band electrons may be captured by both the OH_i and the NBO defects. Similarly, the OH_i may capture a valence hole created by irradiation. If the defect concentration in SiO₂ is low, the charged defects may sustain their charge state until they are neutralized by a conduction electron or valence hole diffusing nearby.

IV. EXPERIMENTS RELATED TO THE 1.9 eV PHOTOLUMINESCENCE BAND IN *a*-SiO₂

In this section we give a summary of the experiments that have been used to support the identification of the defect responsible for the 4.8 eV OA and 1.9 eV PL bands as NBO. We show that all of these observations are consistent with the OH_i -related OA/PL cycle as well.

A characteristic phonon sideband of the zero-phonon line (ZPL) of the 1.9 eV PL band has been observed at 0.11 eV (890 cm⁻¹) beside the main luminescence peak.^{1,2} This ZPL was suggested to be due to Si–NBO stretching vibrations since its frequency is close to the Si–O vibrational frequency in a silanol (Si–OH) complex (969 cm⁻¹) that was observed in Raman spectroscopy.²⁵ Our calculations give 860 cm⁻¹ and 832 cm⁻¹ for the vibrational frequencies of the NBO and Si–OH defects, respectively. The vibrational frequency for silanol has to be smaller than that of the NBO if the O and H oscillate in the same phase, because the mass of the oscillating particle (OH group vs O atom) is larger.

For the calculated Si–O vibrational frequency in the (5)Si–OH⁻ complex we found 845 cm⁻¹ in *a*-SiO₂ in the largest void and 910 cm⁻¹ in α -quartz. Since the (5)Si–OH⁻ behaves in α -quartz similar to smaller voids in the amorphous oxide, we conclude that the ZPL of the OH⁻ related PL falls in the 840–910 cm⁻¹ region, overlapping with what has been obtained for NBO. This result suggests that the

OA/PL cycle originating from both defects is consistent with the ZPL measurement. The site-dependent vibrational energy of the (5)Si–OH⁻ complex gives a contribution to the phonon background of the time-resolved PL spectrum in the ZPL measurement. Shifts in this background should be observable in deuterated oxides since the (5)Si–OD⁻ defect would have a lower vibrational frequency.

The absorption of linearly polarized light in the 4.8 eV band selectively excites defects which have transition dipole moments parallel to the direction of the oscillating electric field (i.e., oriented in the polarization direction of light). The ensemble of these defects produces linearly polarized luminescence at 1.9 eV; however, the polarization direction of the absorbed and emitted light subtends an angle of $\alpha=55.7^\circ$ (Ref. 1).

The transition dipole moment of an optical transition is the integral of the dipole moment operator $e\mathbf{r}$ and can be calculated once the optical matrix elements—and thus the matrix elements of the momentum operator ($-i\nabla$)—are known:

$$\mathbf{r}_{ab} = \langle \Psi_a | \mathbf{r} | \Psi_b \rangle = \frac{\hbar}{im_e} (E_a - E_b) \langle \Psi_a | -i\nabla | \Psi_b \rangle, \quad (2)$$

where transitions occur from state Ψ_b with energy E_b to state Ψ_a with energy E_a .

Let us denote the ground state of the system by $|\Psi_a\rangle$, the excited state with the deep hole by $|\Psi_b\rangle$ and the excited state with the hole at the top of the valence band by $|\Psi_c\rangle$. Then the angle subtended by the absorption and luminescence dipoles is given as

$$\alpha = \arccos \frac{\mathbf{r}_{ab} \cdot \mathbf{r}_{ca}}{|\mathbf{r}_{ab}| \cdot |\mathbf{r}_{ca}|}. \quad (3)$$

For the angle between the OA and PL dipoles we have obtained $\alpha=62^\circ$ for NBO and $\alpha=57^\circ$ for (5)Si–OH⁻ in the large voids of *a*-SiO₂, $\alpha=92^\circ$ for (5)Si–OH⁻ in α -quartz (compare to the experimentally observed value of $\alpha=55.7^\circ$). The results suggest that the angle α in both the NBO and the (5)Si–OH⁻ defects in *a*-SiO₂ is in good agreement with experiment when the system is excited in the 4.8 eV band. The higher angle α in α -quartz is due to the different geometry of the (5)Si–OH⁻ defect caused by the smaller size of the voids. Again, the differences between the results for NBO and (5)Si–OH⁻ are too small to be able to distinguish between the two defects.

If the defect producing the 1.9 eV PL is excited in the 2.0 eV absorption band, the observed angle between the absorption and emission transition dipoles is $\alpha \approx 0$ (Ref. 1). This absorption corresponds to excitations from the valence band edge, i.e., no deep hole is created, therefore electronic relaxations are absent. For both defects, the electron is excited from non-bonding O $2p_z$ orbitals constituting the top of the valence bands to the partially occupied O $2p$ orbital of the NBO or the OH_i , and the luminescence process is exactly the reverse of excitation. In case of the NBO defect no atomic relaxations are present either, so the absorption and emission dipoles would be exactly parallel. For the OH_i however, atomic relaxations will take place even if excitations are

coming from the top of the valence band. The excited and thus negatively charged OH_i molecule moves toward the Si atom before PL, giving rise to a small angle between the absorption and emission dipoles. This increase in the angle α between the transition dipoles with decreasing PL energy has been observed in time-resolved PL polarization spectra upon excitation in the 2.0 eV band.²

The 1.9 eV PL is typically observed at low temperatures (below 110 K).² The disappearing of the PL signal at higher temperatures is explained by the fact that both the NBO and the OH_i are radicals that can easily be passivated by other freely diffusing defects (e.g., hydrogen). Moreover, the OH_i can itself diffuse which, in addition to its high reactivity, is the reason why it was not observed directly in oxides with conventional water content. Assuming that the OH_i is primarily created from interstitial water molecules that mostly reside in the large voids of the oxide, we have calculated the diffusion barrier for an OH_i through a channel connecting two large voids. The obtained 0.3 eV is in excess to the 0.3 eV “binding” energy that arises from a weak dipole interaction between the OH_i and network Si or O atoms (see Sec. III). Therefore, via thermal excitations, the OH_i may become “free” i.e., its weak bond to the network can be disrupted and thereafter it cannot participate in the described optical processes. The energy necessary for breaking the weak bond between the OH_i and the network (0.3 eV) is comparable to the diffusion barrier for interstitial hydrogen (0.2 eV).²⁶ This result shows that both the NBO and the OH_i defects are likely to disappear at the same temperature leading to the vanishing of the PL signature.

Finally, we point out that the red PL from the SiO₂ surface comes entirely from NBO defects²⁷ because (5)Si–OH[−] cannot form at the surface. Since all surface Si atoms are undercoordinated, the addition of an OH[−] group would not make a silicon atom five-fold coordinated.

V. CONCLUSIONS

In summary, we have shown that electronic and atomic relaxations are complementary factors in determining Stokes-shifts at optically active defects in SiO₂. First we have carefully analyzed the NBO defect that has been associated with a 4.8 eV and 2.0 eV OA and 1.9 eV PL band in *a*-SiO₂ and have shown that the large Stokes-shift is entirely due to slow, non-radiative electronic relaxations, in which a deep valence hole, created in the absorption process, “bubbles up” to the valence-band edge by a phonon-assisted mechanism. Using first-principles calculations, we have identified another defect—interstitial OH groups—that have a similar optical signature. For this defect, however, electronic and atomic relaxations are both responsible for the calculated Stokes-shift. The presence of atomic relaxations also introduces site-dependence in the observed optical spectra. Experiments related to the 1.9 eV PL are consistent with both the NBO and OH_i defects.

ACKNOWLEDGMENTS

This work was supported in part by AFOSR Grant No. F-49620-99-1-0289, and by the William A. and Nancy F. McMinn Endowment at Vanderbilt University.

*Present address: Department of Chemical Engineering, University of Massachusetts, Amherst, Massachusetts 01003.

¹L. Skuja, *Solid State Commun.* **84**, 613 (1992).

²L. Skuja, *J. Non-Cryst. Solids* **179**, 51 (1994).

³M. Stapelbroek, D. L. Griscom, E. J. Friebele, and G. H. Sigel, Jr., *J. Non-Cryst. Solids* **32**, 313 (1979).

⁴E. J. Friebele, D. L. Griscom, and M. J. Marrone, *J. Non-Cryst. Solids* **71**, 133 (1985).

⁵G. Pacchioni and G. Ierano, *Phys. Rev. B* **57**, 818 (1998).

⁶T. Bakos, S. N. Rashkeev, and S. T. Pantelides, *Phys. Rev. Lett.* **91**, 226402 (2003).

⁷See e.g., D. W. Hwang, X. F. Yang, S. Harich, J. J. Lin, and X. Yang, *J. Chem. Phys.* **110**, 4123 (1999).

⁸A. A. Wolf, E. J. Friebele, D. L. Griscom, and J. Acocella, *J. Non-Cryst. Solids* **56**, 349 (1983).

⁹M. C. Payne, M. P. Teter, D. C. Allan, T. A. Arias, and J. D. Joannopoulos, *Rev. Mod. Phys.* **64**, 1045 (1992).

¹⁰D. Vanderbilt, *Phys. Rev. B* **41**, 7892 (1990).

¹¹R. Buczko, S. J. Pennycook, and S. T. Pantelides, *Phys. Rev. Lett.* **84**, 943 (2000).

¹²S. N. Rashkeev, D. M. Fleetwood, R. D. Schrimpf, and S. T. Pantelides, *Phys. Rev. Lett.* **87**, 165506 (2001).

¹³T. Bakos, S. N. Rashkeev, and S. T. Pantelides, *Phys. Rev. Lett.*

88, 055508 (2002).

¹⁴D. J. Chadi and M. L. Cohen, *Phys. Rev. B* **8**, 5747 (1973).

¹⁵Y. Tu, J. Tersoff, G. Grinstein, and D. Vanderbilt, *Phys. Rev. Lett.* **81**, 4899 (1998).

¹⁶F. Wooten, K. Winer, and D. Weaire, *Phys. Rev. Lett.* **54**, 1392 (1985).

¹⁷G. Makov and M. C. Payne, *Phys. Rev. B* **51**, 4014 (1995).

¹⁸L. Skuja, *J. Non-Cryst. Solids* **239**, 16 (1998).

¹⁹S. T. Pantelides and W. A. Harrison, *Phys. Rev. B* **13**, 2667 (1976).

²⁰M. Cannas and M. Leone, *J. Non-Cryst. Solids* **280**, 183 (2001).

²¹B. Subramaniam, L. E. Halliburton, and J. J. Martin, *J. Phys. Chem. Solids* **45**, 575 (1984).

²²See, e.g., D. M. Fleetwood, *Microelectron. Reliab.* **42**, 523 (2002).

²³S. M. Sze, *Semiconductor Devices, Physics and Technology* (Wiley, New York, 1985), p. 195.

²⁴S. T. Pantelides, S. N. Rashkeev, R. Buczko, D. M. Fleetwood, and R. D. Schrimpf, *IEEE Trans. Nucl. Sci.* **47**, 2262 (2000).

²⁵C. M. Hartwig and L. A. Rahn, *J. Chem. Phys.* **67**, 4260 (1977).

²⁶B. Tuttle, *Phys. Rev. B* **61**, 4417 (2000).

²⁷Y. Glinka, *J. Exp. Theor. Phys.* **111**, 1748 (1997).